

Mergers of Black Holes in the Galactic Center

F. Elliott Koch and Bradley M.S. Hansen

Department of Physics and Astronomy, University of California, Los Angeles, CA

ABSTRACT

We present the results of three body simulations focused on understanding the fates of intermediate mass black holes (IBH) that drift within the central 0.5 pc of the Galaxy. In particular, we modeled the interactions between pairs of $4000M_{\odot}$ black holes as they orbit a central black hole of mass $4 \times 10^6 M_{\odot}$. The simulations performed assume a Schwarzschild geometry and account for Chandrasekhar dynamical friction as well as acceleration resulting from energy lost due to gravitational radiation. We found the branching ratio for one of the orbiting IBHs to merge with the CBH was 0.95 and is independent of the inner IBH's initial eccentricity as well as the rate of sinking. This, coupled with an infall rate of $\sim 10^7$ yrs for an IBH to drift into the Galactic center, results in an IBH-CBH merger every $\lesssim 11$ Myrs. Lastly we found that the IBH-IBH-CBH triple body system “resets” itself, in the sense that a system with an inner IBH with an initially circular orbit generally left behind an IBH with a large eccentricity, whereas a system in which the inner IBH had a high eccentricity ($e_0 \sim 0.9$) usually left a remnant with low eccentricity. Branching ratios for different outcomes are also similar in the two cases.

Subject headings: black hole physics — Galaxy: center — methods: n-body simulations — relativity

1. Introduction

Starting with the discovery of quasars (Schmidt 1963; Greenstein & Keenan 1964; Greenstein 1964), we have gradually come to appreciate the existence of massive, dark objects in the centers of almost all galaxies (Lynden-Bell 1969; Richstone et al. 1998), although their origins are still unclear. The nature of such a central dark object is best constrained in the center of our own Galaxy. Over the last decade, the infra-red monitoring of the Galactic center has led to severe dynamical constraints on the nature of the Milky Way's central object (Eckart & Genzel 1997; Ghez et al. 1998; Schödel et al. 2002; Ghez et al. 2005), leaving little doubt that it is a black hole with mass $3.7 \pm 0.2 \times 10^6 M_{\odot}$.

An equally interesting result to emerge from these studies is that the stellar population within the central parsec of the galaxy contains an unexpected component of young, massive stars (Sanders 1992; Morris 1993; Genzel et al. 1997; Ghez et al. 2003; Paumard et al. 2006). The origin of these stars is a question of interest because the strong tidal fields close to the central black hole (CBH) are large enough to shear apart a normal molecular cloud at the locations where the stars are seen (Morris 1993). Two principal classes of alternative models have been investigated – one which postulates that the stars form from the gravitational instability of a quasar-like accretion disk around the CBH during an earlier period of high nuclear activity (Levin & Beloborodov 2003) and another which proposes that the stars migrate inwards as part of a stellar cluster which sinks towards the CBH by dynamical friction and is eventually broken up by the strong tidal field (Gerhard 2001). A recent addition to this latter scenario is the possibility that such a cluster contains an intermediate mass black hole (Hansen & Milosavljević 2003), which serves to bind the cluster tighter and slow the internal dynamical relaxation, allowing the cluster to survive long enough to deposit the stars in their observed locations.

Each of these scenarios have their proponents, and the arguments for and against are presented elsewhere (e.g. (Paumard et al. 2006; Berukoff & Hansen 2006)). The goal of this paper is to examine the implications the cluster infall scenario for the merger history of the central black hole. In particular, once the intermediate mass black hole (IBH) is stripped of its coterie of cluster stars, it continues to sink towards the center due to dynamical friction. We wish to examine the final fate of such an IBH and how that fate is reached. We will explore in §2 reasons to believe that the rate of infall of such IBH into the central parsec may actually be larger than the rate at which an individual IBH would merge with the CBH. This then opens the possibility of multiple IBH in orbit, so that in §3 we examine the gravitational interactions of such CBH-IBH-IBH triples and explore the probabilities of various outcomes. The results of this study have a variety of interesting applications, not the least of which is a prediction for the kinds of signals we might expect to observe with future space based gravitational wave observatories. We discuss this further in §5.

2. The fate of a sinking IBH

Let us consider an IBH, surrounded by a handful of stars, the last remnants of the parent cluster, as it sinks towards the CBH. Full dynamical simulations of this scenario can be found in Berukoff & Hansen (2006) but, for our purposes, we consider the simplified model in which the remaining stars have relaxed sufficiently to be distributed in a Bahcall-Wolf density profile ($\propto r^{-7/4}$). We normalise our cluster remnant to contain 50 stars within the

Roche lobe (for a $4000M_{\odot}$ IBH and a CBH mass $4 \times 10^6M_{\odot}$) when located at 1 pc. As the cluster sinks, the Roche lobe shrinks, and stars are stripped and deposited into orbits about the CBH. The last star in this scenario is stripped at separations

$$R_{strip} \sim 0.04pc \left(\frac{\mu}{0.001} \right)^{-1/3} \quad (1)$$

which correspond to angular separations $\sim 1''$. Interior to this radius nearly the entire cluster is stripped, although the full simulations suggest a single closely bound star may be retained. After this, the IBH will sink as an independent, and usually unobservable, entity.

The IBH sinks by dynamical friction – that is, losing energy by scattering stars in the local density field. The sinking will therefore slow when the IBH has sunk far enough that the mass in the potential reservoir of local stars is small compared that of the IBH (Begelman et al. 1980). At this point, the IBH can eject all the available stellar mass without significantly changing its binding energy. Thus, we expect the central region to be largely evacuated of stars, refilled only by dynamical processes that scatter stars inwards from larger radii. The observed density profile of the Galactic center (Genzel et al. 2003) is

$$\rho(R) = 1.2 \times 10^6 M_{\odot} \cdot pc^{-3} \left(\frac{R}{0.4pc} \right)^{-1.4} \quad (2)$$

at distances interior to $R = 0.4pc$. With this profile and our nominal IBH mass of $4000 M_{\odot}$, the ‘stalling radius’ R_{stall} , where the IBH mass equals the mass in field stars interior to that radius, lies at 0.02 pc. Thus, in the simplest version of this scenario, the dynamical drag that drives the IBH inspiral should tail off on scales ~ 0.02 pc, i.e. this is where, in the absence of other effects, the IBH should stall. Such behaviour is, in fact, seen in full N-body simulations of the inspiral process (Matsubayashi et al. 2007; Löckmann & Baumgardt 2007).

Beyond this point, the further evolution of the IBH-CBH binary should follow the kind of pattern outlined by Begelman et al. (1980) for supermassive black hole binaries in galactic nuclei, albeit with a somewhat more extreme mass ratio. The timescale for merger by gravitational wave emission (assuming a circular orbit) from this distance is

$$T_{GW} \sim 10^{14} years \left(\frac{R_{stall}}{0.01pc} \right)^4 \left(\frac{M_{IBH}}{4000M_{\odot}} \right)^{-1} \times \left(\frac{M_{CBH}}{4 \times 10^6 M_{\odot}} \right)^{-2} . \quad (3)$$

On shorter timescales, namely that of the field two-body relaxation time, the stellar loss cone is refilled and the IBH will lose further binding energy in ejecting those stars which cross its orbit. A detailed description of this process is not necessary for our purposes, since

the field relaxation time is $\sim 10^9$ years in the central Galactic parsec, so that the inspiral time is bounded from below by such a timescale.

The reason the long merger times are of interest is because there are several reasons to believe that the interval between IBH deliveries to the central parsec may be considerably shorter than 10^9 years. Perhaps the simplest reason is that, if we take the age of the young massive stars ($\sim 10^7$ years) as a characteristic timescale, then we are faced with the choice between assuming that processes like cluster infall occur regularly on such timescales or assigning a very special and un-Copernican nature to our current epoch. Furthermore, the notion that stellar clusters might contain IBH finds support in the simulations of cluster formation by Portegies Zwart et al. (1999) and Freitag et al. (2006). If the cluster is dense enough, then mass segregation brings massive main sequence stars to the center before they finish their stellar evolution, resulting in an epoch of stellar collisions and mergers. The upshot of this process is the formation of a massive, stellar object a fraction $\sim 10^{-3}$ of the total cluster mass. The subsequent evolution of such an object is far from clear, but unless it manages to lose a considerable fraction of its mass in the form of winds, it is likely to, in the end, form a black hole, since it is far too massive to form either a white dwarf or neutron star.

Of more direct interest to this paper is the calculation of Portegies Zwart et al. (2006), in which they simulate a population of stellar clusters forming in the central 100 parsecs of the Galaxy. They find that $\sim 10\%$ of the clusters born in their simulation will form such IBH progenitors. The result is that IBH sink towards the center with some frequency. Indeed they estimate that the inner 10 pc contains ~ 50 IMBH at any given time and that IBH enter the central parsec every $\sim 10^7$ years. They note that such a high frequency supports the notion (Ebisuzaki et al. 2001) that the CBH may have actually been constructed over a Hubble time via a series of mergers between infalling IBH and a central, growing remnant of such mergers. They also discuss an order-of-magnitude estimate of the merger dynamics, which is the central focus of this paper. We will make a detailed comparison in § 5.

Thus, the scenario we intend to investigate is that in which IBH arrive in the central parsec at intervals $\sim 10^7$ years, but then stall at radii ~ 0.02 pc. As a result, we need to investigate the dynamics of two IBH interacting in the neighbourhood of the CBH.

3. Triple Systems

Assuming that the orbit of an IBH will decay until there is no longer enough stellar mass to affect its orbit, we chose to simulate a three body system consisting of an IBH on a

circular orbit ~ 0.02 pc from the CBH and a second IBH that had started its infall sometime later. The second IBH is introduced at a distance of ~ 0.05 pc and a dynamical friction force is applied to simulate the orbital decay just as the orbit of the inner IBH was assumed to have done. Assuming that these two events are uncorrelated, simulations were repeated for initial orbital plane separations for the two IBHs between 0° and 180° varying in 5° intervals to account for the entire orbital sphere. Therefore without any loss of generality, the initial angle of inclination for the inner IBH (one closest to the CBH) was defined to be zero and the outer IBH was placed randomly on a circular orbit with a semi-major axis of about ~ 0.05 pc in its own orbital plane. A complete statistical ensemble was created by repeating this for 500 relative phases at each angle of inclination between 0 and 180 degrees on 5 degree intervals.

3.1. Integration Algorithm

Integration of the orbits were performed using a Burlisch-Stoer integration algorithm contained in the Mercury6 program written by Chambers (1999). Although the Mercury6 program contains a symplectic integration routines that operate more efficiently and require less overall computational time, the Burlisch-Stoer algorithm more accurately simulates “close encounters” (cases where two masses scatter off of each other) as well as highly eccentric orbits, both of which occur regularly in the results obtained here. The tolerance used to determine each Burlisch-Stoer time step for the integration was set to be $\epsilon = 10^{-15}$ (Press et al. 1997), which was necessary to reduce computational errors caused by the highly elliptical orbits of the IBH on orbits that would graze the CBH, yet still lead to acceptable computing times. The Mercury6 program provided an ideal platform for modeling this system because its primary mode of operation is for simulating the orbital evolution of stellar and planetary systems, and thus the code is optimised to treat the dynamics in the case where the mass is dominated by a single central object. Rescaling the program so that $M_\odot \rightarrow 10^6 M_\odot$ and $1 \text{ AU} \rightarrow 100 \text{ AU}$, the CBH would mimic the central star and the orbiting IBHs would mimic planets. Another useful feature of Mercury6 is that it allows the user to specify a “close encounter” parameter that enables us to monitor scattering events and record the distance of closest approach during IBH-IBH interactions. If the separation of the two black holes was ever smaller than three Hill radii, $a(m_{IBH}/m_{CBH})^{1/3}$, the program would record the time that it occurred and the resulting distance of closest approach. Lastly, the Mercury6 program easily enables the program user to define accelerations due to non-gravitational forces, in this case forces due to dynamical friction and general relativity (see § 3.2 and § 3.3).

3.2. Dynamical Friction

In § 2, we discussed how the orbit of an IBH would decay to an orbital radius where the IBH could no longer eject enough mass to affect the binding energy of its orbit. The dynamical friction force was assumed to be a Chandrasekhar drag force acting on all IBH beyond a radius of $R_{stall} \sim 0.02$ pc from the CBH.

$$\begin{aligned} \frac{d\vec{v}}{dt} &= -4\pi \ln \Lambda G^2 \rho M_{IBH} \\ &\times \left[\operatorname{erf}(X) - \frac{2X}{\sqrt{\pi}} e^{-X^2} \right] \frac{\vec{v}}{v^3} \end{aligned} \quad (4)$$

Where $X \equiv v/\sqrt{2}\sigma$, $\ln \Lambda$ is the Coulomb logarithm, ρ is the background density and σ the velocity dispersion (Binney & Tremaine 1987). Since $Xe^{-X^2} \rightarrow 0$ and $\operatorname{erf}(X) \rightarrow 1$ as $X \rightarrow \infty$ and assuming that ρ and $\ln \Lambda$ change little compared to \vec{v}/v^3 for $R > R_{stall}$ on the time scales we are interested in, then equation (5) can be rewritten as

$$\frac{d\vec{v}}{dt} = -k \frac{\vec{v}}{v^3}. \quad (5)$$

Therefore assuming a density profile similar to that presented by Genzel et al. (2003) and to ensure that $t_{fric} \sim \langle v/\dot{v} \rangle \sim 10^7$ yrs, we set $k \sim \rho M_{IBH} \ln \lambda \sim 10^{-18} \text{ AU}^3/\text{days}^4$. Although t_{fric} is small compared to the relaxation time for the Galactic center, a $t_{fric} \sim 10^7$ yrs was chosen to be consistent with the ages of the young massive stars in the Galactic center (in §5 we briefly discuss results for $t_{fric} \sim 10^6$ yrs and $t_{fric} \sim 10^8$ yrs and note that the final results are well within the measurement error associated with the ensemble size for these simulations). In order to reduce numerical errors associated with crossing into (or out of) the “loss cone”, equation (5) was multiplied by:

$$\kappa = \begin{cases} 0 & \text{if } y \leq 0, \\ \frac{y^2}{2y^2 - 2y + 1} & \text{if } 1 > y > 0, \\ 1 & \text{otherwise} \end{cases} \quad (6)$$

where,

$$y = 4 \frac{r - R_{stall}}{R_{stall}}$$

3.3. General Relativity

Initially our simulations were performed without accounting for any relativistic effects, with the assumption that an ejection from the Galactic center would be the most probable

outcome. We very quickly realized that this was indeed not the case and that relativistic effects must be accounted for. Since we are only interested in the whether or not an IBH merges with the CBH we chose to neglect Post-Newtonian expansions $\lesssim \mathcal{O}(c^{-6})$ which presumably account for plunge and coalescence effects (Blanchet & Iyer 2003). Separating the contributions to the acceleration from the different expansions scaled by multiples of the speed of light, the i^{th} component of the acceleration due to gravity becomes,

$$\frac{dv^i}{dt} = a_0^i + \frac{1}{c^2}a_2^i + \frac{1}{c^4}a_4^i + \frac{1}{c^5}a_5^i \quad (7)$$

where \vec{a}_2 is the $1\mathcal{PN}$, \vec{a}_4 is the $2\mathcal{PN}$ and \vec{a}_5 is the $2.5\mathcal{PN}$ (Kupi et al. 2006). Although there is extensive literature on Post-Newtonian expansions we chose to use the applicable perturbations presented in Damour & Deruelle (1981) and the references cited within (more recent derivations can be found in Itoh et al. (2001) and Blanchet & Iyer (2003)) altered so that the larger of the two masses (the CBH) is defined as the origin of the coordinate system, as in the Mercury code. Using similar arguments presented in Gültekin et al. (2006), Post-Newtonian corrections applied are:

$$\begin{aligned} a_2^i &= \frac{G}{r^2} \left\{ n^i \left[-v^2 5 \left(\frac{GM_{IBH}}{r} \right) \right. \right. \\ &\quad \left. \left. + 4 \left(\frac{GM_{CBH}}{r} \right) \right] + 4v^i n_j v^j \right\}, \end{aligned} \quad (8a)$$

$$\begin{aligned} a_4^i &= \frac{G}{r^2} \left\{ n^i \left[\frac{GM_{IBH}}{r} \left(-\frac{15}{4}v^2 + \frac{39}{2}(n_j v^j)^2 \right) \right. \right. \\ &\quad \left. \left. + 2 \frac{GM_{CBH}}{r} (n_j v^j)^2 \right] - v^i \frac{G}{r} n_j v^j \right. \\ &\quad \left. \times \left(\frac{63}{4}M_{IBH} + 2M_{CBH} \right) \right\} \end{aligned} \quad (8b)$$

$$\begin{aligned} &+ \frac{G^3 M_{CBH}}{r^4} n^i \left(-\frac{57}{4}M_{IBH}^2 - 9M_{CBH}^2 \right. \\ &\quad \left. - \frac{69}{2}M_{IBH}M_{CBH} \right), \\ a_5^i &= \frac{4G^2 M_{IBH} M_{CBH}}{5r^3} \\ &\quad \times \left\{ v^i \left[-v^2 + 2 \frac{GM_{IBH}}{r} \right. \right. \\ &\quad \left. \left. - 8 \frac{GM_{CBH}}{r} \right] + n^i n_j v^j \right. \\ &\quad \left. \times \left[3v^2 - 6 \frac{GM_{IBH}}{r} + \frac{52}{3} \frac{GM_{CBH}}{r} \right] \right\}. \end{aligned} \quad (8c)$$

where \vec{n} is the unit vector pointing towards the CBH and the Einstein summation notation is being used. Averaging changes in the semi-major axis and eccentricity due to the accelerate presented in equation (8d) over orbital periods reproduces the familiar result presented by Peters (1964),

$$\begin{aligned} \left\langle \frac{da}{dt} \right\rangle &= \frac{64 G^2 M_{IBH} M_{CBH} (M_{IBH} + M_{CBH})}{5 c^5 a^3 (1 - e^2)^{7/2}} \\ &\times \left(1 + \frac{73}{24} e^2 + \frac{37}{96} e^4 \right), \end{aligned} \quad (9a)$$

$$\begin{aligned} \left\langle \frac{de}{dt} \right\rangle &= \frac{304 G^2 M_{IBH} M_{CBH} (M_{IBH} + M_{CBH})}{15 c^5 a^4 (1 - e^2)^{5/2}} \\ &\times \left(1 + \frac{121}{304} e^2 \right), \end{aligned} \quad (9b)$$

where a is the semi-major axis and e is the eccentricity (Gültekin et al. 2006).

4. Orbital Characteristics

Using the formalism defined above, we identify three broad categories of orbital history. The most noticeable differences between these regimes are the length of time needed for the system to progress through the different stages, the effect of orbital resonances between the two IBHs and the degree to which the relative inclination varies.

The first category consists of prograde orbits, with a small initial angle of inclination, $0^\circ < \Delta i_0 < 40^\circ$. Figure (1) is a plot of the orbital parameters for both of the IBHs as a function of time for $\Delta i_0 = 10^\circ$. This plot shows that the two IBHs first begin to interact with each other at about 0.5 ± 0.05 Myrs, which is roughly the same for all prograde orbits. The two IBH soon become locked in a 2:1 orbital mean-motion resonance, which leads to the orbit of the inner IBH beginning to decay as well. The overall rate of decay slows, since the strong mutual interaction means that the energy extracted by dynamical friction on the outer IBH is removed from both IBH orbits in concert. In fact, as the evolution proceeds, and the eccentricities of both orbits grow, the apastron of the inner IBH can reach out beyond the evacuated region and thus both IBH experience some measure of dynamical friction. Continued evolution leads to eccentricity growth and eventually, after ~ 4.5 Myr, the eccentricities and inclinations experience large-amplitude variations, leading to instability. The time at which this epoch of strong interactions occurs depends on the initial relative inclination, occurring earlier for larger values of Δi_0 . The two IBH continue to interact until either one is ejected or passes sufficiently close to the CBH that it loses orbital energy to gravitational radiation, resulting in an eventual merger with the CBH.

As Δi_0 increases, the time that elapses before strong interactions occur decreases. This rarely occurs before 2 Myrs for $\Delta i_0 < 40^\circ$. However, for $\Delta i_0 \geq 40^\circ$ (except $\Delta i_0 = 180^\circ$) strong perturbations almost immediately start affecting the orbit, presumably as a result of the Kozai effect (Kozai 1962) (also seen in N-body simulations, e.g. Aarseth (2007)). We classify the orbits with $40^\circ \leq \Delta i_0 \leq 90^\circ$ as our second class of orbital solutions. Figure (2) contains plots of the evolution of orbital parameters for $\Delta i_0 = 40^\circ$ and shows the rapid onset of eccentricity and inclination growth. Like the prograde orbits with $\Delta i_0 < 40^\circ$, a 2:1 orbital resonance is established at about 0.5 Myrs, but shortly afterward, at about 1.5 Myrs, strong oscillations begin to dominate the resonant behavior of the eccentricity and angle of inclination.

In the third regime, $\Delta i_0 > 90^\circ$, strong oscillations in inclination begin almost immediately (figure 3). Additionally, since the two orbits are retrograde with respect to each other, the interaction times are shorter and less frequent, therefore an orbital resonance is more difficult to establish and the exchange of energy through “close encounters” is more important. However, there are clearly still strong oscillations in eccentricity and inclination most likely driven by the Kozai effect (figure 3). Although the result of the simulation is essentially the same as the other initial inclination regimes, how the result is achieved is obviously slightly different.

The three groups of initial angles of inclination differ in the overall time periods associated with the evolution of an IBH’s orbit, but they all result in orbits that transfer angular momenta between the two IBHs as seen through large oscillations in inclination angle and eccentricity of the IBHs’ orbits. Ultimately the transfer of orbital energy and angular momentum between the two IBH results in either an IBH-CBH merger or the ejection of one of the IBH. Mergers generally occur when the resonant interactions drive the eccentricity of one of the IBH to the point where it starts to interact strongly with the CBH near periastron, radiating gravitational waves and resulting eventually in a merger. Ejections occur when the resonant avoidance fails and the two IBH undergo close encounters. Eventually the IBH undergo a close enough passage that one of them is scattered onto a hyperbolic orbit. The end result in both cases is to leave the remaining IBH on an eccentric orbit.

4.1. IBH-CBH Mergers, Ejections and the Orbital Characteristics of the Remaining IBH

Although the majority of IBH-CBH mergers resulted in a gradual transfer and loss of energy such that the remaining IBH was left still orbiting the CBH, there appeared to be a small subset of IBH-CBH mergers, $\lesssim 1\%$, in which the other IBH was unbound. Unlike the

majority of the IBH-CBH mergers (described below), these were the result of an IBH-IBH scattering event that transferred enough energy from one of the IBHs to cause the other to be ejected. The IBH that remained bound was sufficiently eccentric that it radiated the remainder of its orbital energy as gravitational radiation and merged with the CBH.

The eventual outcome of the dynamical interactions is either that one of the IBH is ejected from the immediate vicinity of the CBH, or that one of the IBH merges with the CBH. Typically an IBH-CBH merger is the result of an IBH on a highly eccentric orbit passing too closely to the CBH, whereby orbital energy from the IBH is carried away via gravitational radiation and the IBH spirals down. Prior to the merger, orbital energy and angular momentum are transferred between the two IBHs as they orbit the CBH (and extracted by dynamical friction from the outermost IBH). This transfer of energy and angular momentum cause the eccentricities of the orbits to oscillate. Formally then, each IBH sends a burst of gravitational radiation as they pass through periastron. As the periastron distance starts to approach the CBH, this energy loss becomes significant. Figure (4) is a plot of the average power radiated through gravitational waves and shows this oscillatory behavior. Furthermore, this plot shows that the power radiated increases as the orbits of the IBHs decay. Lastly, to ensure that a IBH-CBH merger wasn't a numerical artifact of the integration, the data in figure (4) was numerically integrated. The resulting energy lost along with the energy lost to dynamical friction was within $0.1 \pm 0.05\%$ of the orbital energy of the IBH that merged.

Surprisingly, the probability of an IBH-CBH merger had essentially no dependence on the initial angle between the orbital planes of the two black holes, with the exception of the geometrically restricted special cases $\Delta i_0 = 0^\circ$ and $\Delta i_0 = 180^\circ$. Figure (5) is a plot of the probability of a merger or ejection occurring, figure (6) the probability of a given IBH either being ejected and (7) the probability of merging with the CBH as a function of inclination angle. The largest out of plane dependence of the branching ratios is associated with $\Delta i_0 = 0^\circ$ and $\Delta i_0 = 180^\circ$, in which case the planar geometry excludes the oscillations in inclination that aid in eccentricity growth (Iwasawa et al. 2005). Although not as dramatic, there appears to be a slight increase (decrease) in the probability of an IBH being ejected from the Galactic center (merging with the CBH) between $\Delta i_0 \sim 20^\circ$ and $\Delta i_0 \sim 50^\circ$, this could be explained by the increased influence of the Kozai effect. In comparing these two special cases, we find it is almost 50% more likely for an ejection to occur for $\Delta i_0 = 180^\circ$ than it is for $\Delta i_0 = 0^\circ$ because an orbital resonance is established for $\Delta i_0 = 0^\circ$, and not for $\Delta i_0 = 180^\circ$, which transfers energy between the two IBHs in such a way that one of the IBH develops a highly eccentric, low periastron orbit when $\Delta i_0 = 0^\circ$. Furthermore, the phase space plots of two separate simulations for the same value of Δi_0 support the belief that ejections are the result of IBH-IBH scattering events and an IBH-CBH merger is the result

of an IBH-IBH orbital resonance (figures 8 and 9). The boxed region in figure (8) shows that the orbital energy of one of the IBH had been changed abruptly giving the IBH access to a previously “forbidden” region. Unlike the phase space diagram for the ejected IBH, figure (9) has clearly defined regions without any abrupt penetration into a “forbidden” region.

The strong mutual interactions between the IBH do not always maintain a strong enough repulsion to prevent close encounters between the IBH. When such close encounters occur, they alter the orbits of the IBH to the point that the resonance interaction is broken. A sequence of close encounters follows until one of the energy exchanges is strong enough to eject one of the IBH from the central parsec, leaving the other bound in an eccentric orbit. However, the three body interaction between the two IBHs and the CBH does not transfer enough energy to the ‘ejected’ IBH such that it is capable of breaking free of the Galactic potential. In fact, the average energy of the ejected IBH was found to be $\sim 6 \times 10^{-11} M_{\odot} c^2$. Crudely accounting for dynamical friction the IBH would then begin another infall at $\sim 5 - 10$ pc, thereby returning to the inner 0.05 pc of the Galactic center ~ 100 Myr assuming a comparable t_{fric} used in our calculations.

Although the majority of all IBH-CBH interactions leave a single IBH in orbit around the CBH, there appeared to be a small subset of IBH-CBH mergers, $\lesssim 1\%$, in which the other IBH was unbound. Unlike the majority of the IBH-CBH mergers (described above), these were most-likely the result of an IBH-IBH scattering event that transferred enough energy from one of the IBHs to cause the other to be ejected. The IBH that remained bound was sufficiently eccentric that it then radiated the remainder of its orbital energy as gravitational radiation and spiraled down to merge with the CBH. Thus, in these rare cases, it is possible to end up with neither of the initial IBH in orbit around the CBH.

Figure (10) is a plot of the distribution of eccentricity of the remaining IBH, for which the average value is 0.676 ± 0.005 , and which is skewed more towards higher eccentricities. Indeed, the majority of orbits have an eccentricity of ~ 0.9 . Additionally, we show the small fraction, $\lesssim 0.1\%$, of cases where the “remaining” IBH had an eccentricity of greater than 1. These were the result of the low probability events mentioned above, in which one IBH is ejected and the other merges with the CBH. In order to test whether or not our initial conditions were a realistic simulation of the system, further simulations of the IBH-IBH-CBH triple system were performed, in which the inner IBH was given an initial orbit with a large eccentricity (~ 0.9). These yielded similar results as before, with the exception that the system evolved much more quickly, taking $\sim 1/10$ the amount of time required when the initial eccentricity of the inner IBH was $\lesssim 0.2$. Furthermore, the average eccentricity of the remaining IBH from these simulations was $\lesssim 0.2$ with the majority of the remaining orbits with an eccentricity < 0.1 (figure 11). This is a consequence of the

fact that, when the inner IBH had a highly eccentric orbit with low pericenter, it was more susceptible to a rapid merger with the CBH, as the initial resonant interactions drive the periastron to smaller values. In these cases, the inner IBH was typically merged with the CBH prior to dramatically affecting the outer IBH’s eccentricity. The cases that resulted in ejections behaved similarly as before, since the mutual close encounters between the IBH quickly erased any memory of the initial conditions. Therefore, even though the remaining IBH after the initial IBH-IBH-CBH system has resulted in either an IBH-CBH merger or IBH ejection may have a highly eccentric orbit, a second IBH-IBH-CBH interaction yields branching ratios for an IBH-CBH merger (or IBH ejection) similar to those that result when starting with a small eccentricity (≤ 0.3) (within statistical error) and will mostly likely lead to initial conditions for the IBH remaining after this IBH-IBH-CBH interaction similar to those of the original scenario. Thus, overall, our simulations yield branching ratios of 0.65 and 0.35 for mergers and ejections respectively (figure 5). Coupling this with an infall rate consistent with the ages of the stars discussed in the introduction, results in an IBH-CBH merger $\lesssim 15$ Myrs, whether the the inner IBH has a small initial eccentricity, $\lesssim 0.3$ or a large initial eccentricity $\gtrsim 0.7$. This supports the idea that supermassive black holes could be created by successive mergers of IBHs over a long period of time. We also found magnitude of the gravitational radiation emitted during the IBH-CBH merger is consistent with Iwasawa et al. (2005) and should be able to be detected by LISA.

5. Discussion

The model problem discussed here was motivated by the desire to understand the consequences of a steady rate of infall of IBH into the Galactic center, a potential consequence of theories for the origins of the young stars observed there. Perhaps surprisingly, we find that the probability of a merger between the CBH and one of the IBH is greater than the probability of an ejection (figure 5). Coupling the observed branching ratio of 0.65 for an IBH-CBH merger, along with the infall rate $\sim 10^7$ yrs (consistent with the ages of the young stars found in the central parsec), results in an IBH-CBH merger occurring approximately once every 11 Myrs. We have also found similar results for both enhanced and reduced dynamical friction ($t_{fric} \sim 10^6$ yrs and $t_{fric} \sim 10^8$ yrs) where the differences are associated with statistical error and the total time for infall and IBH-IBH interactions to occur. Depending on the rate of IBH infall, such mergers may have contributed significantly to the mass growth of the CBH (Ebisuzaki et al. 2001).

The eccentricity of a surviving IBH is determined by several factors. Dynamical friction will circularise the orbit (e.g. Berukoff & Hansen (2006)), although this depends on the

background density profile. Indeed, eccentricity can be pumped if there is an evacuated core, so that dynamical friction operates over only part of the orbit, as we have seen in this calculation and has been verified in numerical simulations such as Löckmann & Baumgardt (2007). In our case, these effects are superceded by the strong interactions between the pair of IBH, both in the form of resonant interactions and close passages and scattering. However, we find that a system that starts with an inner IBH on an eccentric orbit is likely to leave a survivor on a low eccentricity orbit, and vice versa. Taken together, this implies that the outcome of a series of IBH infalls can be considered as a chain of three-body encounters such as the ones described here, unless the rate of infall is considerably faster than one every 10^7 years.

In conclusion, although the stellar scattering responsible for dynamical friction cannot cause an IBH-CBH merger in a Hubble time, the dynamical interactions between two or more IBH result in ejection or merger on timescales $\sim 10^7$ years, so that the number of IBH inhabiting the central parsec today should be small in number, even if the process of infall is a regular feature of Galactic center life.

The authors acknowledge useful conversations with Steve Berukoff regarding his work simulating the scenario feeding our initial conditions and John Chambers regarding the operation of *Mercury6*.

REFERENCES

- Aarseth, S. J. 2007, ArXiv e-prints, 710
- Begelman, M. C., Blandford, R. D., & Rees, M. J. 1980, *Nature*, 287, 307
- Berukoff, S. J. & Hansen, B. M. S. 2006, *Cluster Core Dynamics at the Galactic Center*
- Binney, J. & Tremaine, S. 1987, *Galactic dynamics* (Princeton, NJ, Princeton University Press, 1987), 424
- Blanchet, L. & Iyer, B. R. 2003, *Classical and Quantum Gravity*, 20, 755
- Chambers, J. E. 1999, *MNRAS*, 304, 793
- Damour, T. & Deruelle, N. 1981, *Physics Letters A*, 87, 81
- Ebisuzaki, T., Makino, J., Tsuru, T. G., Funato, Y., Portegies Zwart, S., Hut, P., McMillan, S., Matsushita, S., Matsumoto, H., & Kawabe, R. 2001, *ApJ*, 562, L19

- Eckart, A. & Genzel, R. 1997, MNRAS, 284, 576
- Freitag, M., Rasio, F. A., & Baumgardt, H. 2006, MNRAS, 368, 121
- Genzel, R., Eckart, A., Ott, T., & Eisenhauer, F. 1997, MNRAS, 291, 219
- Genzel, R., Schödel, R., Ott, T., Eisenhauer, F., Hofmann, R., Lehnert, M., Eckart, A., Alexander, T., Sternberg, A., Lenzen, R., Clénet, Y., Lacombe, F., Rouan, D., Renzini, A., & Tacconi-Garman, L. E. 2003, ApJ, 594, 812
- Gerhard, O. 2001, ApJ, 546, L39
- Ghez, A. M., Duchêne, G., Matthews, K., Hornstein, S. D., Tanner, A., Larkin, J., Morris, M., Becklin, E. E., Salim, S., Kremenek, T., Thompson, D., Soifer, B. T., Neugebauer, G., & McLean, I. 2003, ApJ, 586, L127
- Ghez, A. M., Klein, B. L., Morris, M., & Becklin, E. E. 1998, ApJ, 509, 678
- Ghez, A. M., Salim, S., Hornstein, S. D., Tanner, A., Lu, J. R., Morris, M., Becklin, E. E., & Duchêne, G. 2005, ApJ, 620, 744
- Greenstein, J. L. 1964, ApJ, 140, 666
- Greenstein, J. L. & Keenan, P. C. 1964, ApJ, 140, 673
- Gültekin, K., Miller, M. C., & Hamilton, D. P. 2006, ApJ, 640, 156
- Hansen, B. M. S. & Milosavljević, M. 2003, ApJ, 593, L77
- Itoh, Y., Futamase, T., & Asada, H. 2001, Phys. Rev. D, 63, 064038
- Iwasawa, M., Funato, Y., & Makino, J. 2005, ArXiv Astrophysics e-prints
- Kozai, Y. 1962, AJ, 67, 591
- Kupi, G., Amaro-Seoane, P., & Spurzem, R. 2006, MNRAS, 371, L45
- Levin, Y. & Beloborodov, A. M. 2003, ApJ, 590, L33
- Löckmann, U. & Baumgardt, H. 2007, ArXiv e-prints, 711
- Lynden-Bell, D. 1969, Nature, 223, 690
- Matsubayashi, T., Makino, J., & Ebisuzaki, T. 2007, ApJ, 656, 879
- Morris, M. 1993, ApJ, 408, 496

- Paumard, T., Genzel, R., Martins, F., Nayakshin, S., Beloborodov, A. M., Levin, Y., Trippe, S., Eisenhauer, F., Ott, T., Gillessen, S., Abuter, R., Cuadra, J., Alexander, T., & Sternberg, A. 2006, *ApJ*, 643, 1011
- Peters, P. C. 1964, *Physical Review*, 136, 1224
- Portegies Zwart, S. F., Baumgardt, H., McMillan, S. L. W., Makino, J., Hut, P., & Ebisuzaki, T. 2006, *ApJ*, 641, 319
- Portegies Zwart, S. F., Makino, J., McMillan, S. L. W., & Hut, P. 1999, *A&A*, 348, 117
- Press, W. H., Teukolsky, S. A., Vetterling, W. T., & Flannery, B. P. 1997, *Numerical Recipes in C: The Art of Scientific Computing* 2nd Ed. (Cambridge University Press), 724–729
- Richstone, D., Ajhar, E. A., Bender, R., Bower, G., Dressler, A., Faber, S. M., Filippenko, A. V., Gebhardt, K., Green, R., Ho, L. C., Kormendy, J., Lauer, T. R., Magorrian, J., & Tremaine, S. 1998, *Nature*, 395, A14+
- Sanders, R. H. 1992, *Nature*, 359, 131
- Schmidt, M. 1963, *Nature*, 197, 1040
- Schödel, R., Ott, T., Genzel, R., Hofmann, R., Lehnert, M., Eckart, A., Mouawad, N., Alexander, T., Reid, M. J., Lenzen, R., Hartung, M., Lacombe, F., Rouan, D., Gendron, E., Rousset, G., Lagrange, A.-M., Brandner, W., Ageorges, N., Lidman, C., Moorwood, A. F. M., Spyromilio, J., Hubin, N., & Menten, K. M. 2002, *Nature*, 419, 694

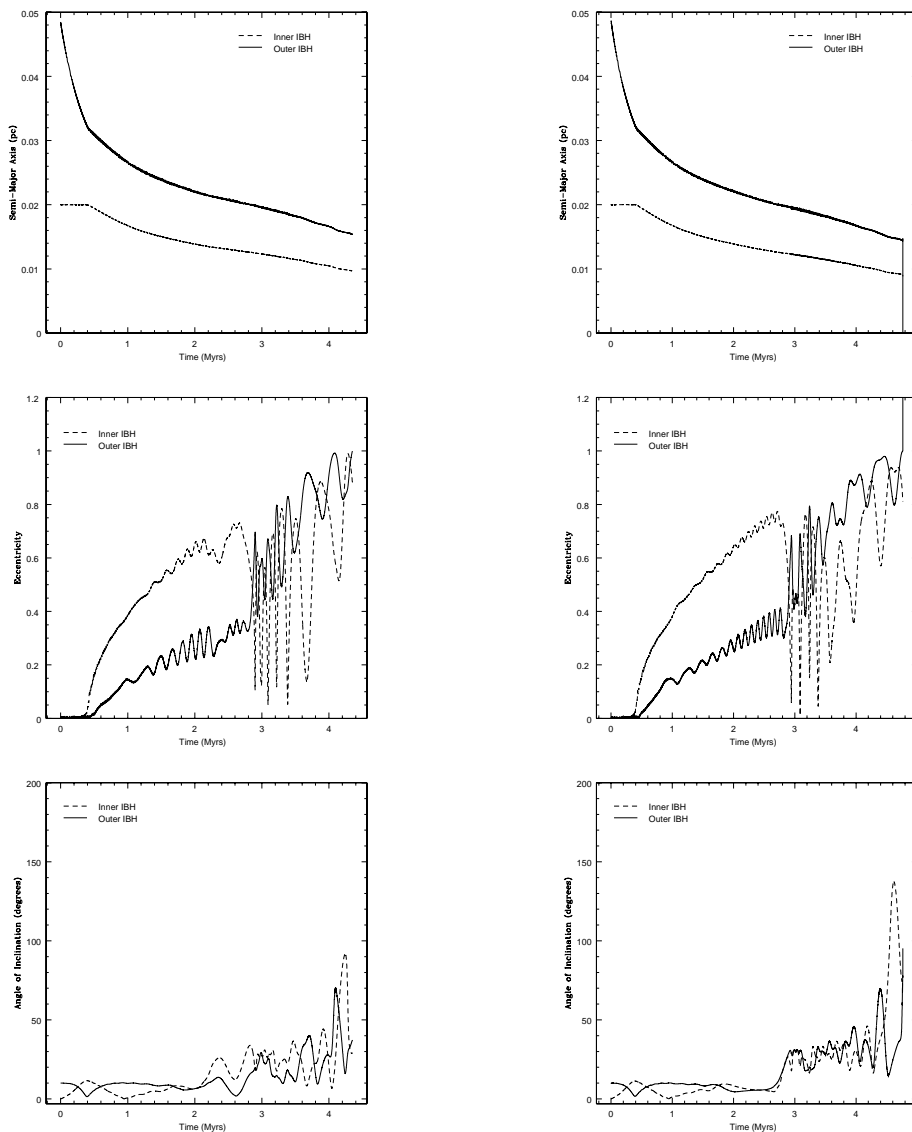


Fig. 1.— Orbital parameters, semi-major axis (upper left merged, upper right ejected), eccentricity (middle left merged, middle right ejected) and angle of inclination (lower left merged, lower right ejected) as a function of time for $\Delta i_0 = 10^\circ$. The result of these simulations were that the outer IBH merged with the CBH for plots on the left and the outer IBH was ejected beyond 4 pc for plots on the right.

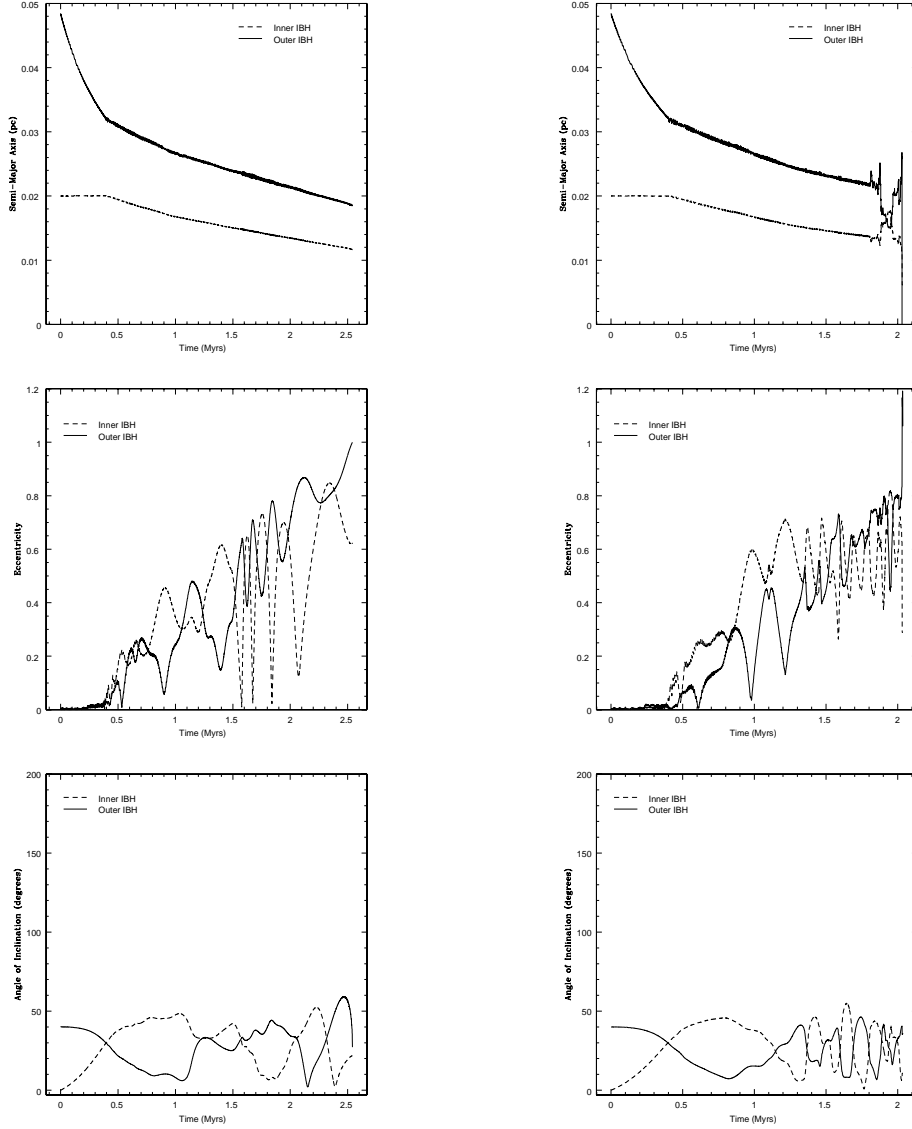


Fig. 2.— Orbital parameters, semi-major axis (upper left merged, upper right ejected), eccentricity (middle left merged, middle right ejected) and angle of inclination (lower left merged, lower right ejected) as a function of time for $\Delta i_0 = 40^\circ$. The result of these simulations were that the outer IBH merged with the CBH for plots on the left and the outer IBH was ejected beyond 4 pc for plots on the right.

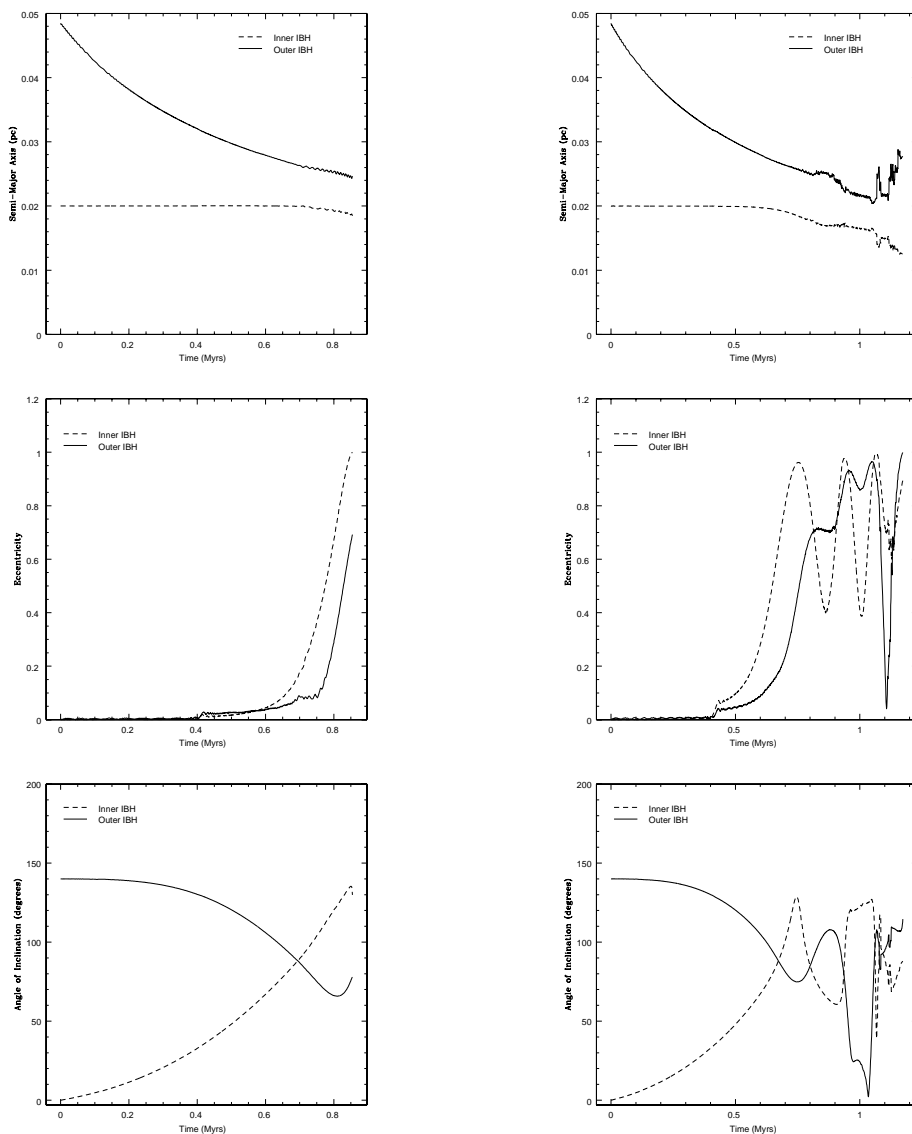


Fig. 3.— Orbital parameters, semi-major axis (upper left merged, upper right ejected), eccentricity (middle left merged, middle right ejected) and angle of inclination (lower left merged, lower right ejected) as a function of time for $\Delta i_0 = 140^\circ$. The result of these simulations were that the inner IBH merged with the CBH for plots on the left and the outer IBH was ejected beyond 4 pc for plots on the right.

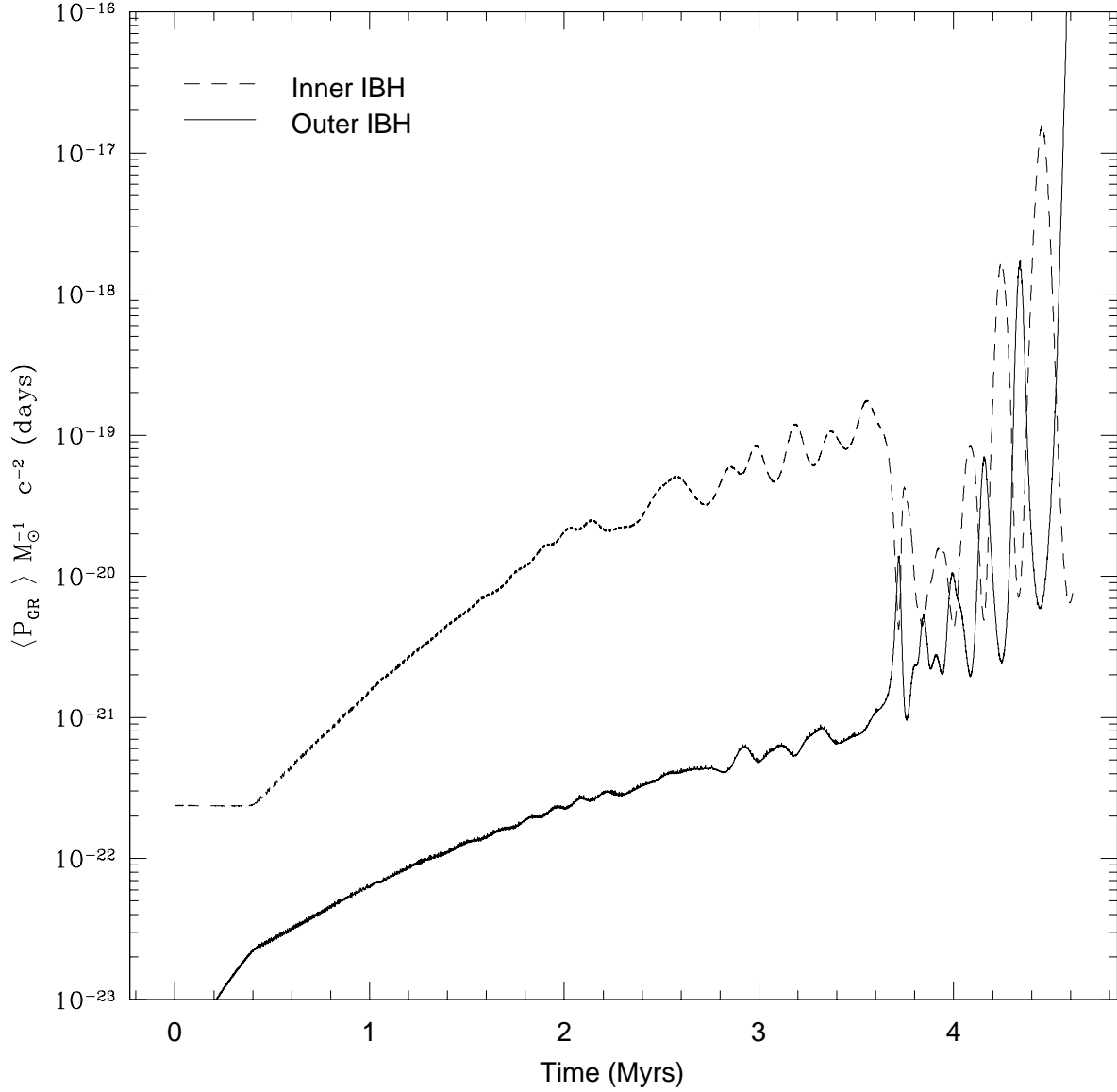


Fig. 4.— Normalised power radiated by gravitational radiation, $\langle P_{GR} \rangle / M_{\odot} c^2$, as a function of time in Myrs for the two IBH. Although this particular plot is associated with an IBH-CBH merger with $\Delta i_0 = 10^\circ$ (orbital parameters shown in figure 1), it is a good representation of the typical power radiated as the IBH-IBH-CBH three body system evolves, regardless of the final outcome. The oscillatory behaviour of $\langle P_{GR} \rangle / M_{\odot} c^2$ corresponds with the transfer of angular momentum as well as orbital energy between the two IBHs. As their eccentricities grow and periapsis decreases, more and more energy is radiated away until there is one last, large release of energy before the IBH-CBH merger occurs.

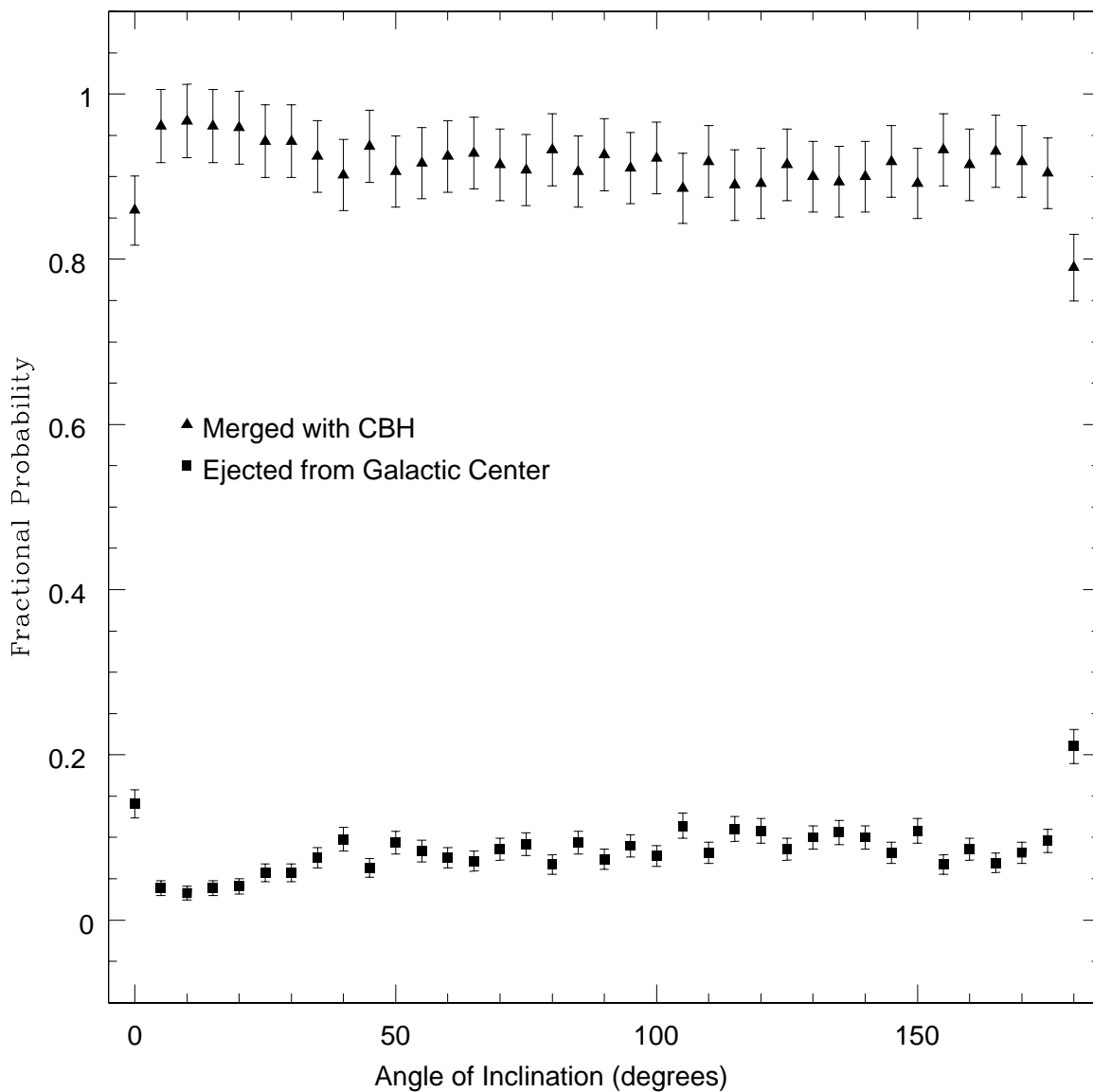


Fig. 5.— Branching ratios as a function of initial relative angle of inclination angle between the two IBH, Δi_0 . These probabilities correspond with the case of the inner IBH initially having a circular orbit, although subsequent simulations with the initial eccentricity of the inner IBH equal to 0.2, 0.3, 0.6 and 0.9 resulted in probabilities within the error of those presented above.

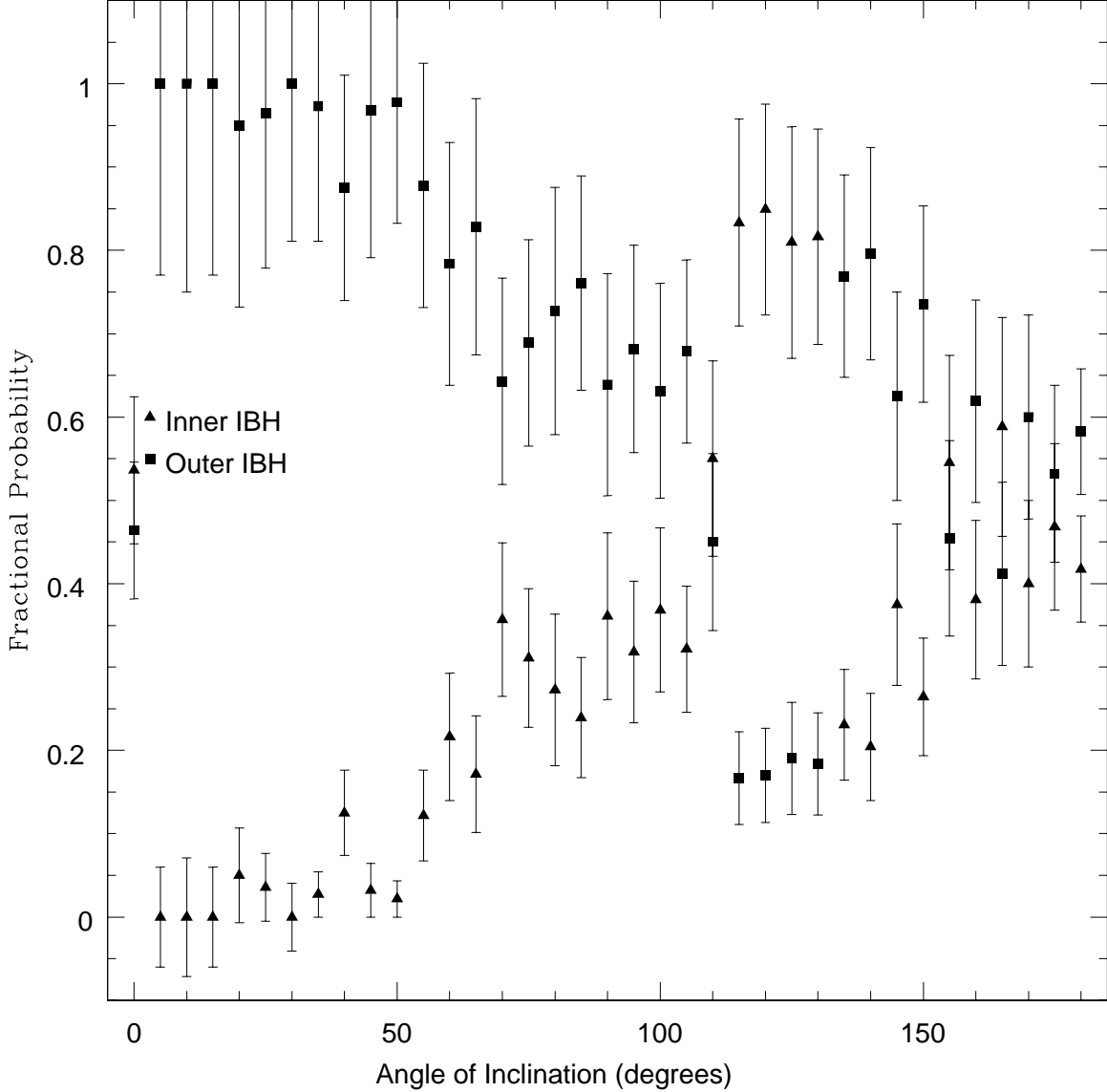


Fig. 6.— Probabilities with which a given IBH (either inner or outer) was ejected, plotted as a function of the initial relative angle of inclination, Δi_0 . For values of Δi_0 less than 75° the outer IBH had a greater probability for being ejected than the inner IBH. As $\Delta i_0 \rightarrow 90^\circ$, the probability that the outer IBH decreases until the two IBH have essentially an equal probability of being ejected. As the initial orbits become retrograde with respect to each other the inner IBH has a slightly greater probability of being ejected which slowly decreases as $\Delta i_0 \rightarrow 180^\circ$

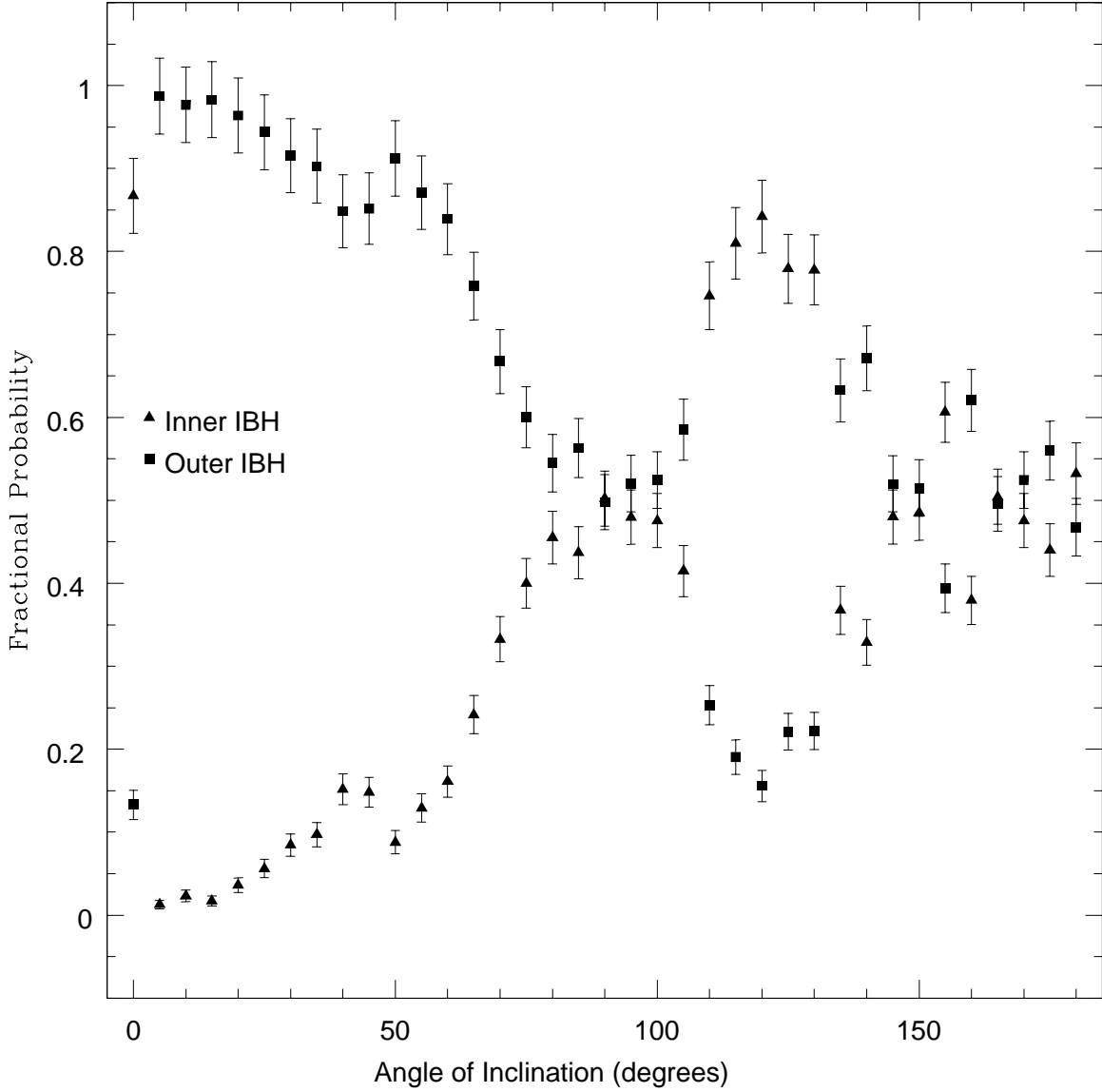


Fig. 7.— Probabilities of which IBH (initially inner or outer) that merged with the CBH plotted as a function of the initial relative angle of inclination, Δi_0 . Surprisingly, much like the ejection probabilities plotted in figure (6), the outer IBH is most likely to merge with the CBH for $\Delta i_0 < 75^\circ$. Unlike the probability with which IBH is ejected, there is a more distinct transition at $\Delta i_0 = 90^\circ$ where the inner IBH becomes more likely to merge with the CBH. Lastly, as $\Delta i_0 \rightarrow 180^\circ$ the two IBH essentially have the same probability of merging with the CBH.

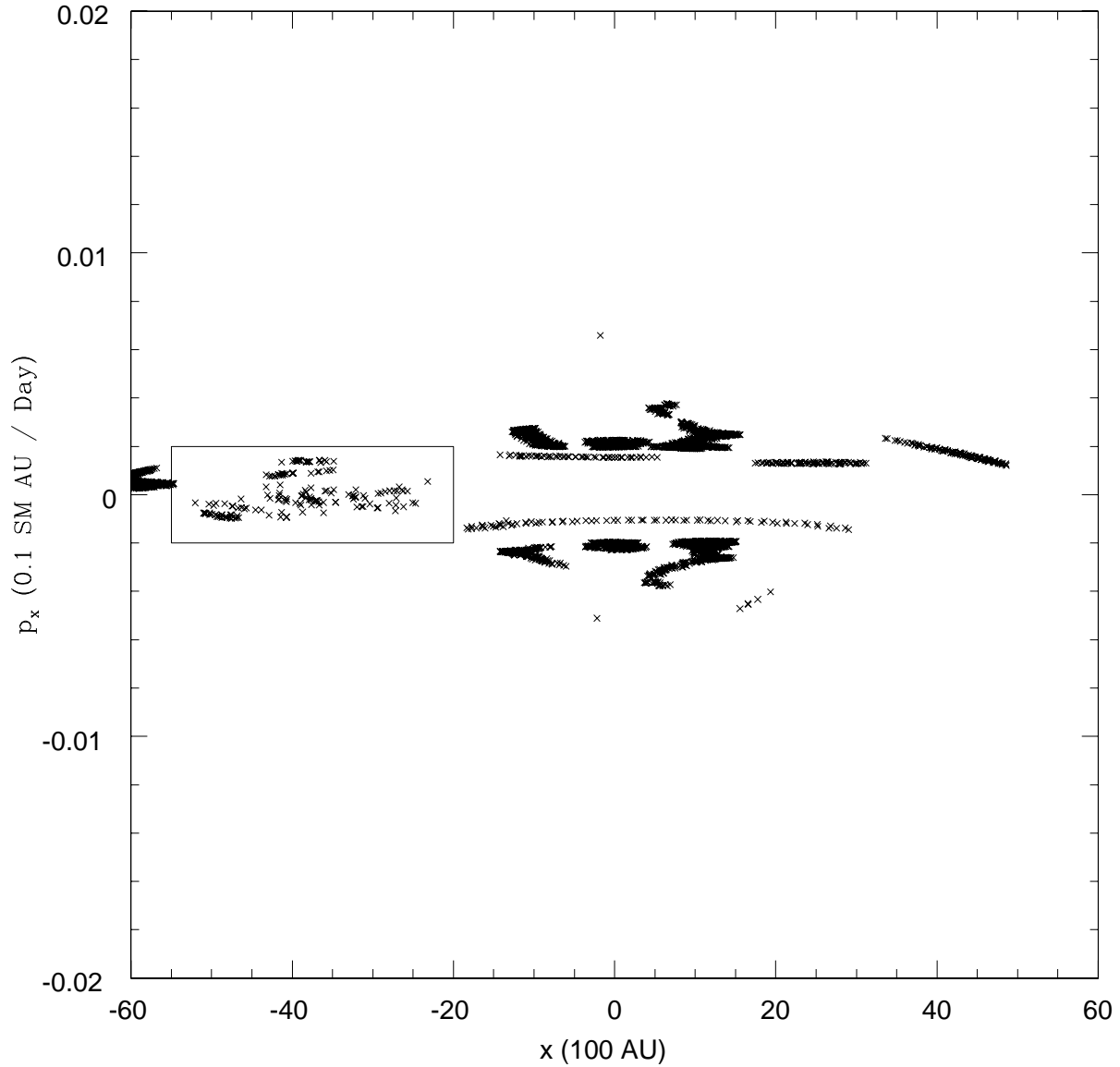


Fig. 8.— Phase space diagram (momentum and position for a fixed axis) for an integration resulting in the ejection of the outer IBH. Although the dynamical friction and to a lesser extent, general relativistic effects, "smear" the phase space plot, the boxed region shows behavior consistent with orbital scattering.

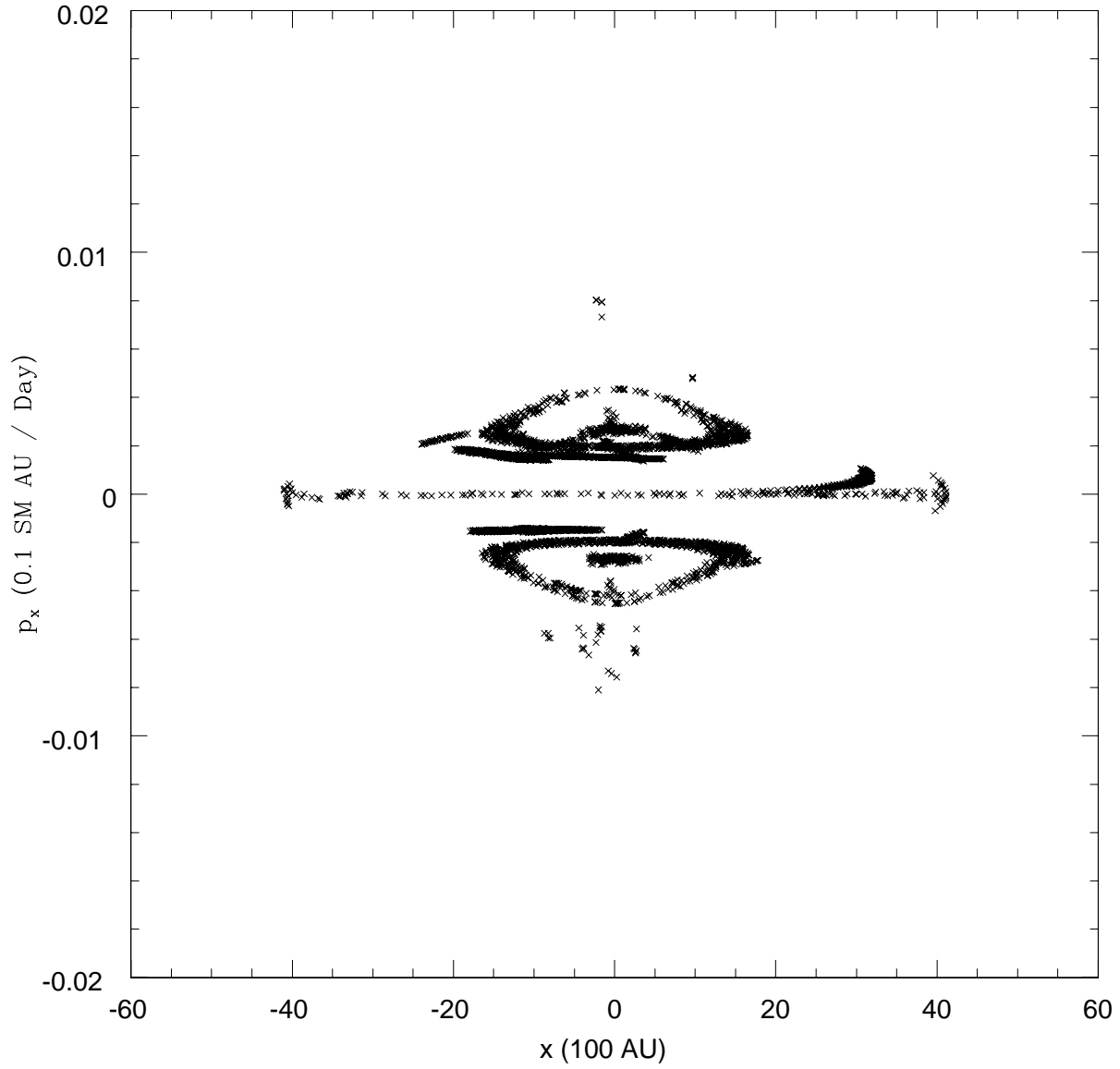


Fig. 9.— Phase space diagram for an integration resulting in an IBH-CBH merger. Unlike figure 8, the only "smearing" of the phase space plot is due to dynamical friction and relativistic effects.

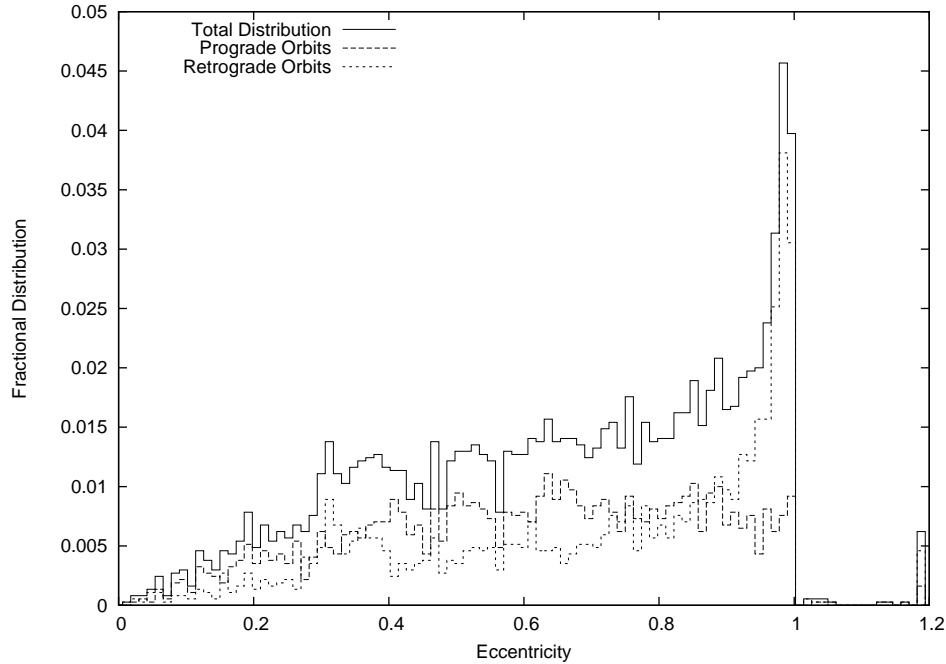


Fig. 10.— Distribution of the eccentricity of the remaining IBH. Note that all eccentricities greater than 1.2 were binned as having an eccentricity of 1.2. These are highly improbable, occurring $\lesssim 0.1\%$ of the time and are the result of an IBH-IBH interaction that ejected one IBH (the “remaining” IBH) where the other IBH lost enough energy to have an orbit close enough to the CBH to radiate its remaining orbital energy via gravitational radiation. Additionally, notice that $\gtrsim 80\%$ of the final eccentricities greater than 0.8 are associated with retrograde orbits.

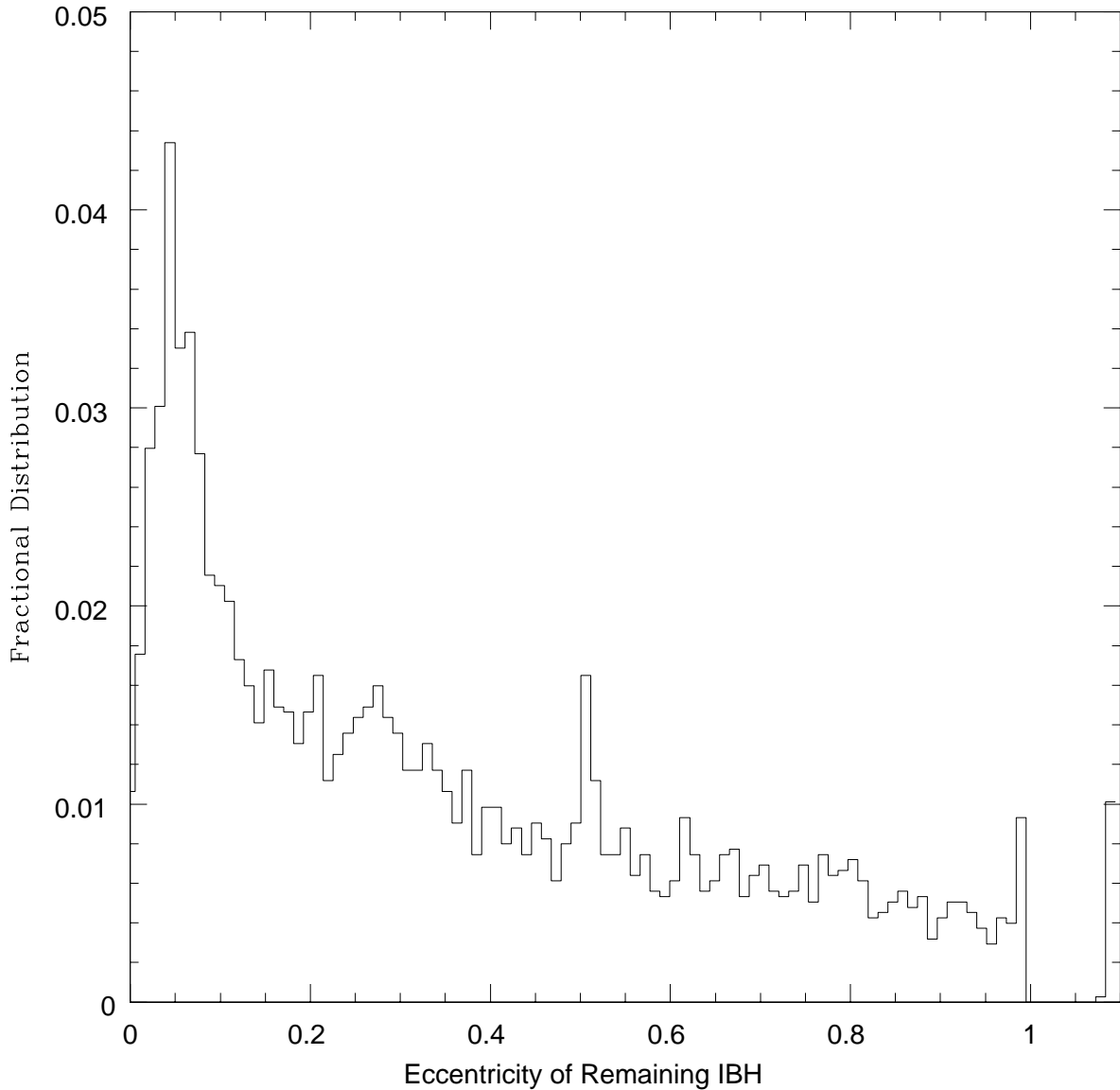


Fig. 11.— Distribution of the eccentricity of the remaining IBH where the initial eccentricity of the inner IBH was 0.9. Although the average eccentricity of the remaining IBH is ~ 0.46 , the most probable eccentricity is ~ 0.05 which implies that after a third IBH falls into the inner parsec, the system is essentially back to the original configuration. Furthermore, the distribution of eccentricities ≥ 1.1 were combined and are the result of an IBH-CBH merger that was caused by a dramatic transfer of energy ejecting the other IBH. Lastly, the probability of merger or ejection is not affected by the large initial eccentricity of the inner IBH.